Role of Hydrogen Bonding to Bound Dioxygen in Soybean Leghemoglobin†

H. Caroline Lee,*,‡ Jonathan B. Wittenberg,§ and Jack Peisach‡,§

Departments of Molecular Pharmacology and of Physiology and Biophysics, Albert Einstein College of Medicine, Yeshiva University, Bronx, New York 10461

Received June 17, 1993; Revised Manuscript Received August 19, 1993•

ABSTRACT: Electron spin echo envelope modulation (ESEEM) spectroscopy was applied to oxy cobaltous soybean leghemoglobin (oxyCoLb) in D_2O at various pH values to investigate electron nuclear superhyperfine coupling to N_ϵ of the proximal histidyl imidazole and to exchangeable deuterons. Two spectroscopically distinct forms of oxyCoLb, acid and neutral, were identified. In the acid form, a 0.82-MHz hyperfine coupling to ^2H was found, indicating the presence of a hydrogen bond to bound O_2. No hyperfine-coupled ^2H was found in the neutral form. Nuclear hyperfine and nuclear quadrupole couplings to the proximal histidyl N_ϵ in the acid form are smaller than those in the neutral form: A_{iso} = 2.22 MHz and e^2qQ = 1.98 MHz for the acid form; A_{iso} = 2.90 MHz and e^2qQ = 2.22 MHz for the neutral form. The differences are believed to result from the presence of a hydrogen bond to bound O_2 in the acid form. A discussion of the contribution of this hydrogen bond to the pH-dependent O_2 affinity of leghemoglobin is presented.

Two histidine residues are conserved in the active site of most known O_2-carrying hemoproteins (Hunt et al., 1978; Dickerson & Geis, 1983). The first, the proximal histidine, is ligated to the heme iron at one of the axial coordination positions and provides the only covalent protein linkage to the heme. The second, the distal histidine, is close enough to the O_2 binding site to be a hydrogen-bond donor to the bound O_2. Since this His···O_2–Fe–His unit is common to most oxy globins, it is of interest to characterize its electronic structure and correlate this with functional properties. A common method for studying electronic structures of metalloproteins is EPR[1] spectroscopy. However, this method cannot be used to study native oxy globins since they contain a diamagnetic metal center.

Paramagnetic analogues of globins can be prepared by substitution of the heme with CoPPIX (Hoffman & Petering, 1970), which, like FePPIX, binds O_2 reversibly. The metal center of oxy Co globins can be described electronically as Co^{3+}–O_2^- • ($S = {}^1/_2$), with the bulk of the unpaired electron spin density on the bound O_2 (Hoffman et al., 1970). This distribution of electron spin density not only generates a paramagnetic prosthetic group in the hemoprotein but also allows for the use of ESEEM spectroscopy, a pulsed EPR technique, to investigate electron nuclear hyperfine coupling to (i) the N_ϵ of the proximal histidine (Magliozzo et al., 1987; Lee et al., 1992) and (ii) exchangeable ^2H in the vicinity of the bound O_2, including those that are hydrogen-bonded to the O_2 ligand (Lee et al., 1992). Thus the application of ESEEM spectroscopy to oxy Co globins makes it possible to monitor simultaneously interactions between the metal center and the two conserved histidines.

In a recent study, ESEEM spectroscopy was used to demonstrate the presence of a hydrogen bond to bound O_2 in oxyCoMb (Lee et al., 1992). The presence of this hydrogen bond was found to reduce electron nuclear superhyperfine coupling to the proximal histidyl N_ϵ in oxyCoMb relative to that in oxyCo *Glycera* Hb (Lee et al., 1992), which does not have a hydrogen-bond donor to the O_2 ligand in the distal heme pocket (Arents & Love, 1989). In the present work, this *trans* effect is investigated in another oxy Co-substituted globin, soybean leghemoglobin a.

Soybean Lbs are monomeric hemoglobins found in nitrogen-fixing root nodules (Appleby, 1984). Among monomeric globins, these proteins have some of the highest O_2 affinities known, which are mainly the result of rapid association and moderately slow dissociation rates (Imamura et al., 1972; Wittenberg et al., 1972; Gibson et al., 1989). This phenomenon may be related to a possible physiological role of maintaining a free O_2 concentration that is low enough to avoid damage to the O_2-sensitive bacterial nitrogenase enzymes in nodules (Gibson et al., 1989).

The high O_2 affinities of Lbs have generated much interest in understanding their structures. The major Lb from soybean, Lb a, studied in this work, has an amino acid sequence (Hunt et al., 1978) and three-dimensional structure (Ollis et al., 1983) resembling those of sperm whale Mb and a-chains of human Hb. The position of the distal histidine, His 61, in Lb is analogous to that of His 64 in sperm whale Mb (Ollis et al., 1983), and like His 64 in sperm whale Mb (Phillips & Schoenborn, 1981), His 61 in Lb may serve as a hydrogen-bond donor to bound O_2. The proposed hydrogen bond between *protonated* His 61 and bound O_2 has been used to explain pH-dependent changes in functional and spectroscopic characteristics of oxyFeLb and oxyCoLb, such as O_2 dissociation rates (Wittenberg et al., 1972; Appleby et al., 1983; Gibson et al., 1989; Martin et al., 1990; Ikeda-Saito et al., 1981), as well as NMR (Johnson et al., 1978; Appleby et al., 1983), optical (Fuchman & Appleby, 1979; Appleby et al., 1983), and EPR (Ikeda-Saito et al., 1981) spectral properties. These pH-dependent characteristics of Lb make it an excellent system for investigating the effect of distal hydrogen bonding on the proximal axial imidazole ligand, a *trans* effect, in an oxy globin without the need for a natural or engineered mutant.

† This work was supported by N.I.H. Grants GM40168 and RR02538 (to J.P.) and NSF Grant DCB-9017722 (to J.B.W.). J.B.W. is a Research Career Awardee 1-K6-733 of the U.S. Public Health Service, National Heart, Lung and Blood Institute.

* Author to whom correspondence should be addressed.

‡ Department of Molecular Pharmacology.

§ Department of Physiology and Biophysics.

• Abstract published in *Advance ACS Abstracts*, October 1, 1993.

[1] Abbreviations: CW, continuous wave; EPR, electron paramagnetic resonance; ESEEM, electron spin echo envelope modulation; FT, Fourier transform; Hb, hemoglobin; IR, infrared; Lb, leghemoglobin; Mb, myoglobin; NMR, nuclear resonance; NQI, nuclear quadrupole interaction; PPIX, protoporphyrin IX; RR, resonance Raman; TPP, tetraphenylporphyrin.

0006-2960/93/0432-11500$04.00/0

We present an ESEEM study of oxyCoLb (i) to demonstrate the presence of a hydrogen bond to the bound O_2 at a acidic pH and (ii) to examine the effect of this hydrogen bond on the nuclear hyperfine and nuclear quadrupole coupling to the proximal histidine. These structural analyses allow for a discussion of the relationship of the electronic structure and O_2-binding kinetics of CoLb and FeLb.

MATERIALS AND METHODS

Protein Preparation. Soybean Lb α was prepared by the method of Appleby et al. (1975). Extraction of heme (Yonetani, 1967) and reconstitution with CoPPIX (Yonetani et al., 1974) followed published procedures. No ion-exchange chromatography was carried out subsequent to the Sephadex column chromatography.

EPR and ESEEM samples were prepared by mixing one part protein (v/v) with two parts buffer and then freezing in liquid nitrogen in air. The buffers used were 50–100 mM citrate (pH 4), MES (pH 6), and bicine (pH 8). Deuterated buffers contained 60–80 atom % ^{2}H. pH meter readings of deuterated buffers were not corrected for isotope effects. Protein concentrations were approximately 1 mM.

Spectroscopy. CW EPR spectra were EPR spectra were recorded at 77 K on a Varian E112 spectrometer equipped with a Systron-Donner frequency counter.

ESEEM data were recorded at liquid helium temperatures (1.4–4.2 K) on a pulsed EPR spectrometer previously described (McCracken et al., 1987), using both transmission cavities (Mims, 1974) and folded stripline cavities (Britt & Klein, 1987) that can accommodate 4 mm o.d. EPR tubes. Three-pulse, or simulated echo, experiments (Peisach et al., 1979) were conducted at microwave frequencies between 8.6 and 10.2 GHz. The time intervals between the first and the second pulses, τ, was chosen as multiples of the proton Larmor frequency in order to suppress modulations from weakly coupled ^{1}H (Peisach et al., 1979). Data were collected at the time $2\tau + T$, where T was the time interval between the second and the third pulses. Each data set contained 1024 points; each point respresented the average of 40–150 measurements of the integrated electron spin echo amplitude. The spectra presented are Fourier transformations of the time domain data after dead time reconstruction (Mims, 1984).

Computer Simulation. CW EPR spectra were simulated using a modified version of the program QPOWA (Belford & Nilges, 1979; Maurice, 1981; Nilges, 1979) with line widths of 25, 15, and 15 MHz in the x, y, and z directions, respectively.

The computer program for simulation of ESEEM spectra has been described previously (Cornelius et al., 1990). The input parameters for a simulation are (i) the principal values of the g and ^{59}Co ($I = {}^7/_2$) nuclear hyperfine tensors, obtained from simulation of frozen solution CW EPR spectra; (ii) experimental parameters including microwave frequency, magnetic field strength, and the τ value; and (iii) parameters for the ^{14}N spin Hamiltonian:

$$\hat{\mathbf{H}}_N = -g_N\beta_N\mathbf{BI} + \mathbf{SA}_N\mathbf{I} + (e^2qQ/4)[3I_z^2 + 2 + \eta(I_x^2 - I_y^2)] \quad (1)$$

The first, second, and third terms represent respectively the nuclear Zeeman, nuclear hyperfine, and nuclear quadrupole interactions. The nuclear hyperfine tensor, $\mathbf{A}_N$, is described by an isotropic nuclear hyperfine coupling constant, A_{iso}, an effective dipole–dipole distance, r, and two angles, θ and ϕ, that relate the orientations of the nuclear hyperfine and the g tensors. The NQI is described by a nuclear quadrupole coupling constant, e^2qQ, an asymmetry factor, η, and three Euler angles, α, β, and γ, that relate the orientations of the NQI and the g tensors. In a typical simulation, input parameters for ^{14}N nuclear hyperfine and NQI are varied until simultaneous fits are obtained for data collected at three experimental g values (1.99, 2.03, and 2.08).

All simulations were performed on a Microvax II computer.

RESULTS

^{14}N Superhyperfine Coupling in OxyCoLb. The unpaired electron in the metal center of oxy Co globins resides mainly on the O_2 ligand, and yields a free radical type EPR spectrum centered around $g \approx 2$ (Hoffman et al., 1970). Only hyperfine couplings to the ^{59}Co nucleus are resolved. Interaction between the unpaired electron and a ^{14}N nucleus directly coordinated axially to Co gives rise to modulations in the electron spin echo envelope. This assignment is based on ESEEM studies of oxyCoTPP–imidazole and –pyridine model compounds using ^{15}N substitutions (Magliozzo et al., 1987). In oxy Co globins, the coupled nitrogen that gives rise to the ESEEM data is N_ϵ of the proximal histidyl imidazole (Lee et al., 1992).

The ESEEM spectrum of oxy Co globins is typical of that of an electron spin $S = {}^1/_2$ system coupled to a nuclear spin $I = 1$ system (Mims & Peisach, 1978) at conditions of near "exact cancelation" (Flanagen & Singel, 1987) where the magnitude of nuclear hyperfine interaction is close to twice that of the nuclear Zeeman interaction (eq 1). This condition is often met for Cu(II)–imidazole models and copper proteins where ESEEM spectra arise from coupling of the unpaired electron to the amino (remote) ^{14}N of bound imidazole (Mims & Peisach, 1978; Jiang et al., 1990). The ESEEM spectra of systems at near "exact cancelation" normally consist of three sharp, low-frequency lines and a broad, high-frequency line. The low-frequency lines arise from that electron spin manifold where the nuclear Zeeman and the nuclear hyperfine interactions nearly cancel each other. The positions of these lines are thus determined mainly by the NQI. The broad, high-frequency line arises from the other electron spin manifold where the nuclear Zeeman interaction adds to the nuclear hyperfine interaction. In this case, a $\Delta m_I = 2$ transition is observed.

Figure 1 shows the pH dependence of the ESEEM spectra of oxyCoLb in H_2O. At pH 4.3 (spectrum A) and pH 8.2 (spectrum C), oxyCoLb exhibits the four-line ESEEM spectrum described above. ESEEM components are resolved at 0.47, 1.26, 1.75, and 4.56 MHz at pH 4.3 and 0.47, 1.45, 2.13, and 5.36 MHz at pH 8.2. At an intermediate pH, 6.1 (spectrum B), the spectrum contains components found at both pH 4.3 and 8.2.[2] Analogous pH-dependent spectral changes have been observed in NMR and optical spectra of oxyFeLb ($pK \approx 5.3$) (Appleby et al., 1983) and in EPR spectra of oxyCoLb ($pK \approx 5.7$) (Ikeda-Saito et al., 1981). The two spectroscopically distinct forms of oxyCoLb identified by ESEEM will be refered to as the "acid" and the "neutral" forms in the ensuing discussions.

Computer simulation of ESEEM spectra was used to calculate the superhyperfine coupling parameters of the proximal histidyl N_ϵ in the acid and the neutral forms of oxyCoLb. Input g and ^{59}Co hyperfine values (given in the caption for Figure 2) were obtained by simulation of frozen solution CW EPR spectra (Figure 2)(Christahl et al., 1981;

[2] Not all features were resolved at a single τ value.

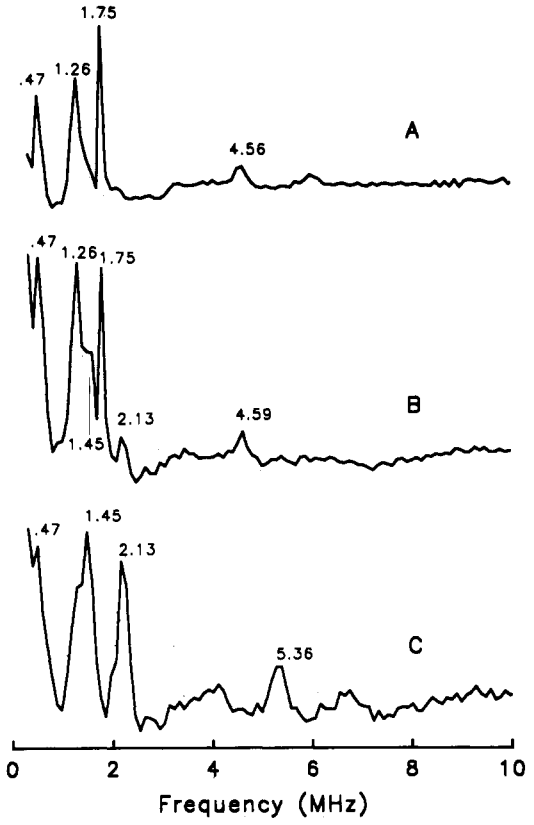

FIGURE 1: ESEEM spectra of oxyCoLb in (A) 67 mM citrate buffer, pH 4.3, (B) 50 mM phosphate buffer, pH 6.1, and (C) 80 mM bicine, pH 8.2. Experimental conditions were (A) frequency = 8.9353 GHz, magnetic field = 3209 G, τ = 146 ns, temperature = 4.2 K; (B) frequency = 8.9371 GHz, magnetic field = 3208 G, τ = 146 ns, temperature = 4.2 K; (C) frequency = 8.9317 GHz, magnetic field = 3207 G, τ = 146 ns, temperature = 4.2 K.

Ikeda-Saito et al., 1981).[3] Simulated ESEEM spectra are shown in Figure 3.[4] Superhyperfine coupling parameters are summarized in Table I. Nuclear hyperfine and nuclear quadrupole coupling parameters for the proximal histidyl N_ϵ are larger in the neutral form than in the acid form.

^{2}H Hyperfine Coupling in OxyCoLb. Two types of exchangeable deuterons in the vicinity of bound O_2 can be detected by ESEEM. The first type consists of those on solvent and ionizable side chains of nearby amino acids that are dipole-coupled to the electron spin. These will give rise to modulations described by the deuterium nuclear Zeeman energy only and will appear at the Larmor frequency in the FT spectrum. The second type consists of those deuterons that are hyperfine-coupled to the electron spin. The ESEEM frequencies of these ^{2}H components are given by

$$\nu(^2\mathrm{H}) = \nu_{\mathrm{Larmor}}(^2\mathrm{H}) \pm {}^1/_2|A_{\mathrm{eff}}| \qquad (2)$$

where $|A_{\mathrm{eff}}|$ is mainly determined by the nuclear hyperfine coupling constant since the ^{2}H quadrupole coupling is expected to be too small to contribute to the spectrum (Mims & Peisach, 1989).

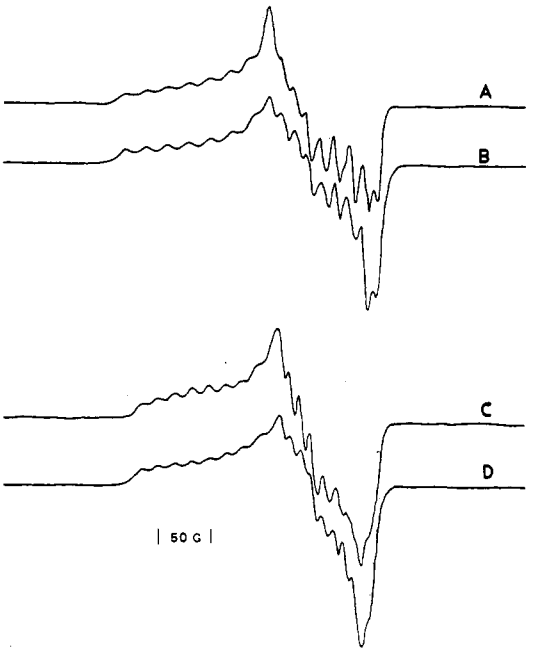

FIGURE 2: Frozen solution CW EPR spectra of oxyCoLb in 67 mM citrate, pH 4.4, D_2O: (A) data, (B) simulation using g_x = 2.0755, g_y = 2.0020, g_z = 1.9875, and A_x^{Co} = 59.83 MHz, A_y^{Co} = 35.08 MHz, A_z^{Co} = 25.00 MHz. Frozen solution CW EPR spectra of oxyCoLb in 67 mM bicine, pH 8.3, D_2O: (C) data, (D) simulation using g_x = 2.0760, g_y = 2.0030, g_z = 1.9890, and A_x^{Co} = 50.84 MHz, A_y^{Co} = 28.21 MHz, A_z^{Co} = 21.01 MHz. Experimental conditions were microwave frequency = 9.12 GHz, microwave power = 5 mW, modulation amplitude = 5 G, temperature = 77 K.

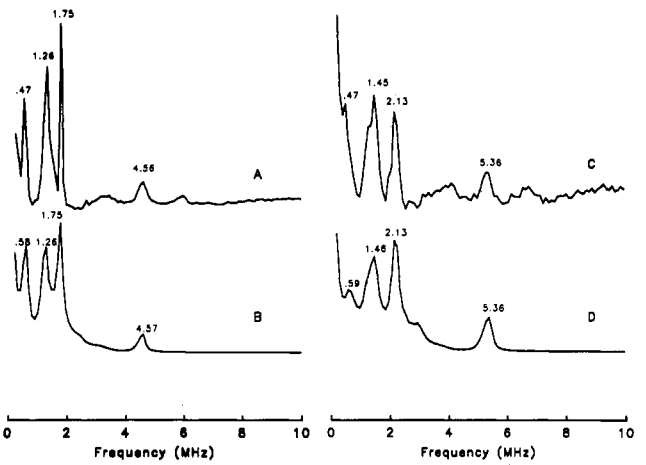

FIGURE 3: ESEEM spectra of the acid form of oxyCoLb: (A) data, (B) simulation using A_{iso} = 2.22 MHz, e^2qQ = 1.98 MHz, η = 0.4, r = 3.6 Å, $\theta = \phi = \alpha = \beta = \gamma = 0°$. ESEEM spectra of the neutral form of oxyCoLb: (C) data, (D) simulation using A_{iso} = 2.90 MHz, e^2qQ = 2.22 MHz, η = 0.5, r = 3.6 Å, $\theta = \phi = \alpha = \gamma = 0°$, β = 40°. Experimental conditions for (A) were the same as those for Figure 1A; for (C), the same as those for Figure 1C.

In addition to the features assigned to the proximal histidyl N_ϵ (Figure 1A), the ESEEM spectrum of the acid form of oxyCoLb in D_2O (Figure 4A)[5] contains two extra components at 2.08 and 2.49 MHz. At the experimental magnetic field setting, 3209 G, the ^{2}H Larmor frequency is 2.08 MHz. This spectral component is assigned to dipole-coupled ^{2}H on solvent

[3] The pH-dependent shift in g values found in the frozen solution EPR spectra of oxyCoLb is consistent with measurements at 15 °C by Ikeda-Saito et al. (1981). Note that the ordinate of Figure 4 in that work should be I_g = 2.033/I_g = 2.038.

[4] The simulation of the ESEEM spectrum of the neutral form shown in Figure 3D utilized r = 3.6 Å and Θ = 0°, same as those used for simulation of the ESEEM spectrum of the acid form (Figure 3B), in order to facilitate a more direct comparison of the ^{14}N superhyperfine coupling parameters. The ESEEM spectrum of the neutral form of oxyCoLb can also be satisfactorily simulated using A_{iso} = 3.10 MHz, θ = 60°, and r = 3.4 Å.

[5] The τ value used to generate the spectrum shown in Figure 4A was different from that used in Figure 1A. For this reason, the relative intensities of ^{14}N components in the two spectra are different.

Table I: Superhyperfine Parameters of Oxy Co Globins

Co protein	A_{eff},[a] ^2H (MHz)	A_{iso},[b] N_ϵ (MHz)	e^2qQ,[b] N_ϵ (MHz)	η[b]
Lb, acid	0.80	2.22	1.98	0.40
Lb, neutral		2.90	2.22	0.30
Mb[c]	0.60	2.46	2.15	0.40
Gly Hb[c]		3.70	2.70	0.50

[a] Equation 2. [b] Uncertainties are A_{iso}, ±0.02 MHz; e^2qQ, ±0.04 MHz; η, ±0.05. [c] Lee et al. (1992).

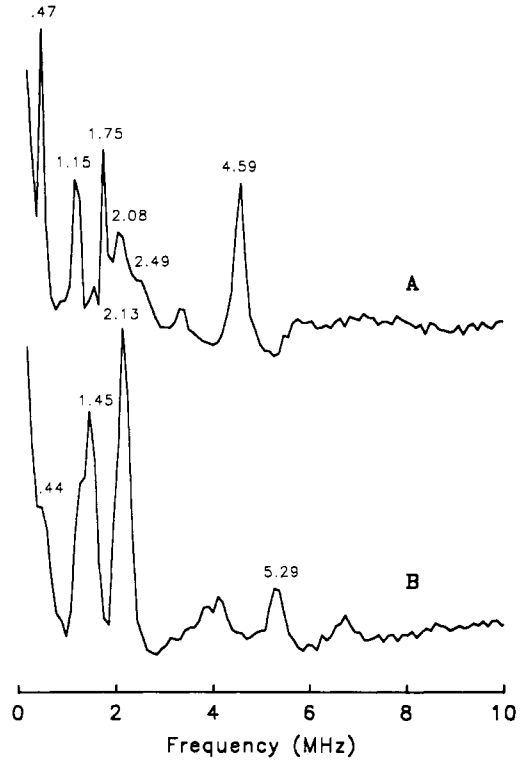

FIGURE 4: ESEEM spectrum of (A) the acid form and (B) the neutral form of oxyCoLb in D_2O. Experimental conditions were (A) 67 mM citrate buffer, 60 atom % ^2H, frequency = 8.9379 GHz, magnetic field = 3209 G, τ = 220 ns, temperature = 4.2 K; (B) 80 mM bicine, 80 atom % ^2H, frequency = 8.9373 GHz, magnetic field = 3209 G, τ = 146 ns, temperature = 4.2 K.

or ionizable side chains of nearby amino acids. The 2.49-MHz component is offset from the Larmor frequency by 0.41 MHz. This line is assigned to ^2H which is hyperfine-coupled to the electron spin with a coupling constant (A_{eff}) of 0.82 MHz.

The ESEEM spectrum of the neutral form of oxyCoLb in D_2O (Figure 4B) contains the same number of components as that in H_2O (Figure 1C). The major difference between the two spectra, recorded at the same τ value, is the large increase, in the D_2O spectrum (Figure 4B), in the intensity of the 2.13-MHz component. This large increase in intensity indicates contribution of dipole-coupled ^2H to the spectrum, since 2.13 MHz is close to the ^2H Larmor frequency at the experimental magnetic field setting. Unlike the acid form of oxyCoLb in D_2O, no ^2H component other than that at the ^2H Larmor frequency is found.

The D_2O experiments were repeated at other microwave frequencies to verify the assignment of spectral components arising from ^2H. When ESEEM data of the acid form were collected at 10.11 GHz, at a field setting of 3629 G (Figure 5A), two broad peaks were resolved at 2.40 and 2.75 MHz. These two peaks are displaced +0.32 and +0.26 MHz, respectively, from their counterparts in the spectrum measured

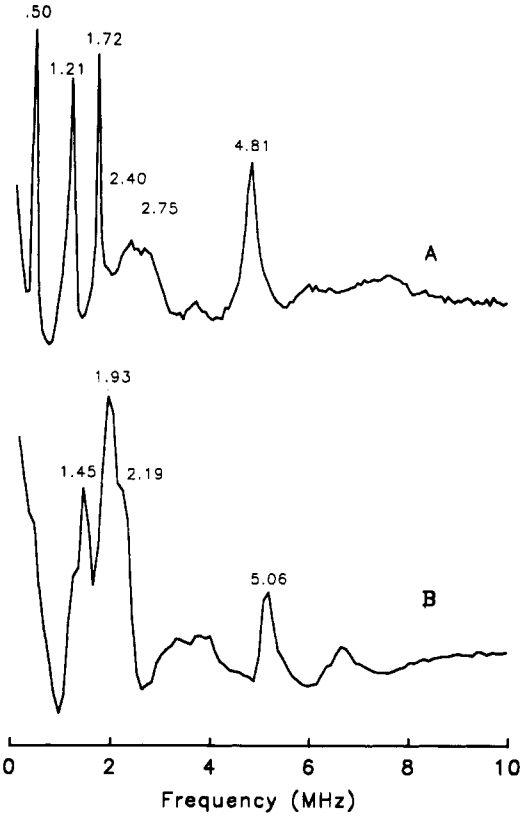

FIGURE 5: (A) ESEEM spectrum of the acid form of oxyCoLb in D_2O. Experimental conditions were microwave frequency = 10.11 GHz, magnetic field = 3629 G, τ = 194 ns, temperature = 4.2 K. (B) ESEEM spectrum of the neutral form of oxyCoLb in D_2O. Experimental conditions were microwave frequency = 8.6781 GHz, magnetic field = 2981 G, τ = 151 ns, temperature = 1.4 K.

at 8.94 GHz and 3209 G (Figure 4A). The shifts in frequency are close to the change in ^2H Zeeman energy (0.27 MHz), thus confirming their assignment as arising from ^2H. For the neutral form, an experiment was repeated at a lower microwave frequency because the presence of a ^{14}N spectral line at 2.13 MHz makes observation of ^2H components (ΔE_{Zeeman} = 0.6536 MHz/kG) more difficult with an increase in magnetic field strength. Data collected at 8.68 GHz and 2981 G (Figure 5B) showed a peak at 1.93 MHz, which is the ^2H Larmor frequency at the experimental magnetic field setting.

The 0.82-MHz ^2H coupling found for the acid form of oxyCoLb was observed at g = 1.99 and 2.03. At g = 2.08, a ^2H component was observed at +0.25 MHz from the Larmor frequency, suggesting an anisotropic ^2H hyperfine coupling. Hyperfine coupling to exchangeable ^2H in oxyCoMb (Lee et al., 1992) and ^1H in oxyCoHb (Höhn & Hüttermann, 1982) were found to be invariant at different magnetic field settings across the EPR spectrum, suggesting that the couplings contain large contact contribution. On the other hand, the nearly isotropic g tensor of oxyCo globins can also prevent observation of anisotropy in ^2H (or ^1H) hyperfine coupling. The results found for oxyCoLb suggest that it is indeed possible to observe anisotropic hyperfine coupling to ^2H in these systems and thus the observed isotropic ^2H coupling in oxyCoMb (Lee et al., 1992) may indeed contain a large contact contribution.

Using a dipole formulation, Höhn and Hüttermann (1982) estimated the magnitude of ^1H hyperfine coupling for oxyCoHb at the three principal values of the g tensor which were determined by single-crystal EPR for oxyCoMb (Dickinson & Chien, 1981). (No single-crystal EPR data for oxyCoHb were available and the values for oxyCoMb were used in their analysis.) Their calculation found that ^1H

hyperfine coupling maximized at g_{max} and g_{mid} and vanished at g_{min}, although they were not able to observe anisotropy in the hyperfine coupling experimentally. Dickinson and Chien (1981) assigned g_{max} for oxyCoMb as the axis closest to the direction of the O–O bond, while an analogous study of Hori et al. (1980) assigned g_{min} as the axis closest to the O–O bond. One would expect to find the largest hyperfine coupling to $^1H/^2H$ along the g axis closest to the direction of the O–O bond since the bulk of the unpaired electron spin density is on the O_2 ligand. For oxyCoLb, although there is no single-crystal EPR or X-ray crystallographic data, it is likely that the g axis closest to the O–O bond is near $g = 1.99$, the field position where the largest ^2H hyperfine coupling in D_2O-exchanged samples is observed by ESEEM. This finding would support the assignment of Hori et al. (1980) of g_{min} as the axis closest to the direction of O–O bond, provided that oxyCoMb and oxyCoLb have analogous structures.

DISCUSSION

Hydrogen Bonding to Bound O_2 in OxyCoLb. Interests in structural studies of Lb arise partially from the pH dependence of its O_2 affinity. Spectroscopic studies of both oxyFeLb and oxyCoLb (Johnson et al., 1978; Fuchman & Appleby, 1979; Appleby et al., 1983; Ikeda-Saito et al., 1981) suggest a pH-dependent structural change that originates from interaction between bound O_2 and exchangeable ^1H in the distal heme pocket, since the deoxy proteins do not exhibit comparable changes with pH. These results are corroborated by our ESEEM study of oxyCoLb. The detection of a 0.82-MHz coupled ^2H in a D_2O-exchanged sample at acidic pH, and its absence at neutral pH, is consistent with a pH-dependent hydrogen bond to the bound O_2. The unpaired electron of oxyCoLb is essentially on the O_2 ligand (Hoffman et al., 1970; Getz et al., 1975; Tovrog et al., 1976; Dedieu et al., 1976). Therefore, a ^2H in oxyCoLb that is coupled to the electron spin with a hyperfine coupling constant of 0.82 MHz is attributable only to those deuterons located in the distal heme pocket and not covalently attached to the bound O_2 (Lee et al., 1992).

Two distal residues, His 61 (E7) and Tyr 30 (B10), have been shown by X-ray crystallography (Ollis et al., 1983) to be potential hydrogen-bond donors to the heme-bound nicotinate in ferric Lb nicotinate. One of them can also be a potential hydrogen-bond donor to heme-bound O_2 in oxy Lb. Since the observed p*Ks* for O_2 affinity and spectroscopic changes for oxyLb are between 5.3 (Appleby et al., 1983) and 5.7 (Ikeda-Saito et al., 1981), similar to the solution p*K* of histidyl imidazole, these changes are likely to be associated with a hydrogen bond between bound O_2 and *protonated* His 61, rather than Tyr 30.

The crystal structure of ferric Lb nicotinate (Ollis et al., 1983) can be used as a model to understand the nature of the hydrogen bond between the distal histidine and bound O_2 in oxyCoLb (Figure 6) and oxyFeLb. In the nicotinate complex, the N_δ of the distal histidine is proposed as the hydrogen-bond donor to the negatively charged carboxylate group of heme-bound nicotinate. Assuming that the position of the distal histidine does not alter in oxyFeLb at acidic pH from that of the nicotinate complex, it is likely that bound O_2 is also hydrogen-bonded to the distal histidyl N_δ, rather than N_ϵ as found in oxyFeMb (see below). If the O_2 ligand in oxyFeLb were to hydrogen-bond to the N_ϵ, the Fe–O–O bond would have to be tilted and almost linear, in contrast to the bent geometry proposed for most oxy globins and oxy Fe porphyrin complexes (Pauling, 1964). On the other hand, if the O_2 ligand in oxyFeLb were hydrogen-bonded to N_δ of the distal histidine, the Fe–O–O bond would have the more commonly observed bent structure.

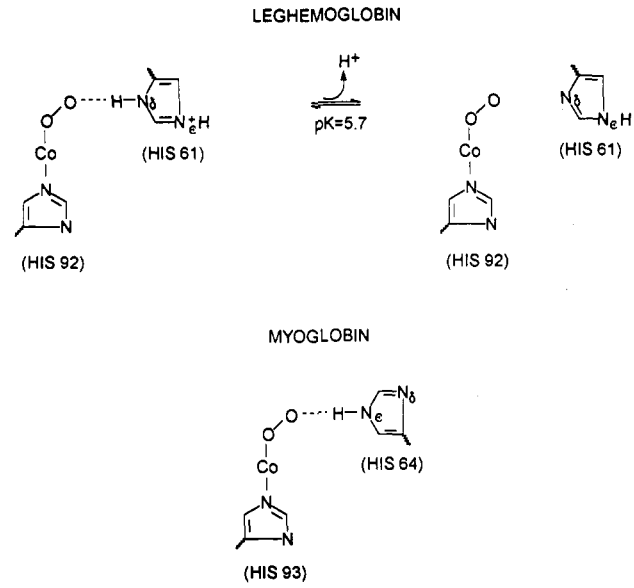

FIGURE 6: Schematic representation the active centers of oxyCoLb and oxyCoMb, indicating different nitrogen atom on the distal histidine serves as hydrogen-bond donor to bound O_2 in the two proteins. The pK given for oxyCoLb is that for the pH-dependent change in the CW EPR of oxyCoLb (Ikeda-Saito et al., 1981).

The distal histidine is conserved in many monomeric globins. In sperm whale Mb, this histidine, His 64, has been shown by a neutron diffraction study in D_2O (Phillips & Schoenborn, 1981) to be the hydrogen-bond donor to bound O_2. A greater ^2H scattering density was found at N_ϵ than at N_δ, thus demonstrating that N_ϵ is the hydrogen-bond donor to the O_2 ligand. This hydrogen bond is present at neutral pH when the distal histidyl imidazole is in the uncharged form and thus contains one exchangeable proton.

Unlike oxyFeMb (Phillips & Schoenborn, 1981) and oxyCoMb (Lee et al., 1992), the hydrogen bond between the distal histidine and bound O_2 in oxyCoLb is shown to be absent at neutral pH (Figure 6). This hydrogen bond is probably also absent in oxyFeLb at neutral pH on the basis of NMR and optical spectroscopic studies (Fuchman & Appleby, 1979; Appleby et al., 1983). This is unusual if one considers the environment of the distal histidine, which has the N_ϵ within hydrogen-bonding or salt bridge formation distance to Lys 57 (E3) (Ollis et al., 1983). One would not expect that any interaction, at neutral pH, between the distal histidine N_ϵ-bound proton and a lysine residue is strong enough to be favored over a hydrogen bond between the distal histidine N_δ and the O_2 ligand, assuming that the position of the distal histidine does not change when the pH is raised to neutrality. In fact, in oxyFeMb at neutral pH, the hydrogen bond between the distal histidine N_ϵ and the O_2 ligand is favored over one between the distal histidine N_δ and solvent (Phillips & Schoenborn, 1981).

Another monomeric globin that exhibits pH-dependent O_2 affinity is lupin Lb II (Gibson et al., 1989). The crystal structure of ferric lupin Lb II nicotinate (Harutyunyan et al., 1980) suggests that, like soybean Lb, the carboxylate group of heme-bound nicotinate forms a hydrogen bond with the N_δ atom of the distal histidine (His 63). A similar bond may also be present between this nitrogen and bound O_2 at low pH, as in the case of oxy soybean Lb discussed above. It is possible that both soybean and lupin II Lb position the distal histidines

in such a way that N_δ is the hydrogen-bond donor and consequently, at neutral pH, when the distal histidyl imidazole is in its uncharged state, the exchangeable ^1H on the imidazole is on N_ϵ and no hydrogen bond to the bound O_2 is possible. Indeed, Pregosin et al. (1971) measured ^{15}N NMR of histidine at acidic pH (0.5–2) when both imidazole nitrogen atoms are protonated. The imidazole ^{15}N chemical shifts are 144.2 and 146.3 ppm, suggesting that the two nitrogens differ in their basicity.

NMR studies of the nicotinate complex of ferric soybean Lb (Trewhella & Wright, 1979, 1980) suggest that heme propionate 7 interacts with the distal histidine, through either a hydrogen bond or a salt bridge, with a $pK \approx 8.3$, although this interaction cannot be confirmed by X-ray crystallography (Ollis et al., 1983) due to low (3-Å) resolution. This proposed heme propionate–distal histidine interaction, if present in oxyFeLb and oxyCoLb, can potentially prevent the formation of a hydrogen bond between the distal histidine and bound O_2 at neutral pH. However, one must also take into consideration the fact that, in ferric lupin Lb II nicotinate (Harutyunyan et al., 1980), heme propionate 7 is hydrogen-bonded to solvent H_2O. Therefore the propionate–distal histidine interaction proposed for oxyFe soybean Lb cannot be responsible for the lack of hydrogen bond to bound O_2 in oxyFe lupin Lb II at neutral pH.

It is unlikely that the absence of a hydrogen bond in oxyFeLb and oxyCoLb at neutral pH is due to movement of the E helix away from the heme such that the distal histidine is too far away to be a hydrogen-bond donor to bound O_2. FeLb has been shown by circular dichroism (Nicola et al., 1975), IR (Fuchman & Appleby, 1979), NMR (Wright & Appleby, 1977; Johnson et al., 1978; Trewhella et al., 1979; Ollis et al., 1981), and EPR (Appleby et al., 1976) spectroscopy to have a flexible heme pocket. In the oxidized protein, the distal histidine can bind to the heme iron at room temperature (Wright & Appleby, 1977) and at cryogenic temperature (Appleby et al., 1976) to form a low-spin ferric complex. Therefore, it is unlikely that there is any structural constraint to prevent the distal histidine from moving close enough to the bound O_2 to form a hydrogen bond.

Superhyperfine Coupling to Proximal Histidine in OxyCoLb. In an ESEEM study of oxyCoMb and oxyCo *Glycera* Hb (Lee et al., 1992), a molecular model (Tovrog et al., 1976) was used to understand superhyperfine coupling in oxyCo globins. It was proposed that the presence of a hydrogen bond to bound O_2 increases the ionic character of the oxyCo unit, leading to a decrease in nuclear hyperfine coupling and in nuclear quadrupole coupling to the proximal histidyl N_ϵ. The results found for oxyCoLb are consistent with this model (Table I).[6] The application of ESEEM to oxy Co globins thus allows for a simultaneous monitoring of the interactions with the two hisidines in the active site. For oxyCoLb, a *trans* effect, the reduction in nuclear hyperfine and nuclear quadrupole coupling to the proximal histidine as a result of hydrogen bonding to the distal histidine, is demonstrated.

Hydrogen Bonding and O_2-Binding Kinetics. The O_2-binding kinetics of several Co globins are summarized in Table II. The hydrogen bond in the acid form of oxyCoLb stablilizes O_2 binding by 3.7 kJ/mol, which is the result of a 3.5-fold decrease in dissociation rate (Ikeda-Saito et al., 1981). An analogous situation is observed when oxyCoMb and oxyCo *Glycera* Hb are compared. The difference in free energy for O_2 binding is 87 kJ/mol, which is mainly the result of a 30-fold difference in dissociation rate. These differences in functional properties in the two systems of comparison are parallelled by the difference in electronic structures in the distal and proximal sides of the CoPPIX prosthetic group. Hyperfine coupling to ^2H on the distal side is accompanied by a reduction of superhyperfine coupling to ^{14}N on the proximal side.

Table II: Kinetic and Equilibrium Constants for Oxygen Binding of Cobalt-Substituted Monomeric Globins

Co proteins	conditions	P_{50}/K_D (Torr)/ (μM)	k_{on} (M^{-1} s^{-1})	k_{off} (s^{-1})
Mb (sperm whale)[a]	pH 7.0, 15 °C	26/70	4×10^7	2.8×10^3
Lb (soybean, α)[b]	pH 4, 15 °C	3.5/6.5	7.4×10^7	4.8×10^2
	pH 8, 15 °C	14.3/23	7.4×10^7	1.7×10^3
Glycera Hb[c]	pH 7.4, 4 °C	700/–		$>8.5 \times 10^4$

[a] Yonetani et al. (1974). [b] Ikeda-Saito et al. (1981). [c] Ikeda-Saito et al. (1977).

Hydrogen bonding to bound O_2 has been used to explain the slow O_2 dissociation rate of oxyMb as compared with its natural (Mims et al., 1983) and engineered (Olson et al., 1988) mutants. This hydrogen bond can also be used to explain the slower O_2 dissociation rate found for the acid form of oxyLb than for the neutral form. However, structural features other than the hydrogen bond to bound O_2 must be considered in order to understand the O_2 binding kinetics of Lb. This becomes apparent when a comparison is extended to the neutral forms of oxyCo (Table II) and oxyFe Lb and Mb. OxyFeMb contains a hydrogen bond to bound O_2 (Phillips & Schoenborn, 1981) and yet exhibits smaller O_2 affinity and faster O_2 dissociation rate (Yamamoto et al., 1974) than the neutral form of oxyFeLb (Appleby et al., 1983), which contains a non-hydrogen-bonded O_2. The same comparison is found for the oxyCo proteins (Table II). This anomaly can arise from differences in the configurations of heme substituents, for example, the vinyl groups (Rousseau et al., 1983), and resultant differences in porphyrin π electron density.[7] Another explanation for the slower O_2 dissociation rate for oxyFeLb (and possible oxyCoLb) is provided by an NMR study (Ollis et al., 1981). Paramagnetic enhancement of acetone (an outer-sphere probe) ^1H relaxation rates in ferric Lb fluoride is less than 50% of that in ferric Mb fluoride, suggesting a less accessible heme pocket in *ligated* forms of Lb than in Mb. This "closed" heme pocket may be responsible for the slow O_2 dissociation rate of oxyFeLb (and oxyCoLb), even in the absence of a hydrogen bond to the bound O_2. In complexes where a hydrogen bond to ligand is believed to be absent, for example, the carbonmonoxy forms, a CO dissociation rate of 0.0068 s^{-1} found for LbCO (Martin et al., 1990), as compared to 0.017 s^{-1} for MbCO (Antonini, 1965) may also be related to a "closed" heme pocket in LbCO.

REFERENCES

Appleby, C. A. (1984) *Annu. Rev. Plant Physiol. 35*, 443.
Appleby, C. A., Nicola, N. A., Hurrell, J. G. R., & Leach, S. J. (1975) *Biochemistry 14*, 4444.
Appleby, C. A., Blumberg, W. E., Peisach, J., Wittenberg, B. A., & Wittenberg, J. B. (1976) *J. Biol. Chem. 251*, 6090.

[6] Hyperfine couplings to ^{14}N estimated by FT EPR techniques (Christahl et al., 1981) are inconsistent with our ESEEM results.

[7] A reviewer suggested that, besides altering the porphyrin π electron density, the orientations of the vinyl groups can also alter the porphyrin nitrogen basicity, and consequently the Lewis acidity of the metal; it is the latter effect that is more directly responsible for change in O_2 binding properties.

Appleby, C. A., Bradbury, J. H., Morris, R. J., Wittenberg, B. A., Wittenberg, J. B., & Wright, P. E. (1983) *J. Biol. Chem. 258*, 2254.
Antonini, E. (1965) *Physiol. Rev. 45*, 123.
Arents, G., & Love, W. E. (1989) *J. Mol. Biol. 210*, 149.
Belford, R. L., & Nilges, M. J. (1979) Presented at the International Electron Paramagnetic Resonance Symposium, 21st Rocky Mountain Conference, Denver, CO.
Britt, R. D., & Klein, M. P. (1987) *J. Magn. Reson. 74*, 535.
Christahl, M., Raap, A., & Gersonde, K. (1981) *Biophys. Struct. Mech. 7*, 171.
Cornelius, J. B., McCracken, J., Clarkson, R. B., Belford, R. L., & Peisach, J. (1990) *J. Phys. Chem. 94*, 6977.
Dedieu, A., Rohmer, M.-M., & Veillard, A. (1976) *J. Am. Chem. Soc. 98*, 5789.
Dickerson, R. E., & Geis, I. (1983) *Hemoglobin: Structure, Function, Evolution, and Pathology*, Benjamin/Cummings Publishing Co., Inc., Menlo Park, CA.
Dickinson, L. C., & Chien, J. C. W. (1980) *Proc. Natl. Acad. Sci. U.S.A. 77*, 1235.
Flanagan, H. L., & Singel, D. J. (1987) *J. Chem. Phys. 87*, 5606.
Fuchsman, W. H., & Appleby, C. A. (1979) *Biochemistry 18*, 1309.
Gibson, Q. H., Wittenberg, J. B., Wittenberg, B. A., Bogusz, D., & Appleby, C. A. (1989) *J. Biol. Chem. 264*, 100.
Getz, D., Melamud, E., Silver, B. L., & Dori, Z. (1975) *J. Am. Chem. Soc. 97*, 3846.
Harutyunyan, E. G., Karanova, L. P., Tovbis, A. B., Grebenko, A. I., Voronova, A. A., Nekrasov, Yu. V., & Vainshtein, B. K. (1980) *Sov. Phys.–Crystallogr. 25*, 302.
Hoffman, B. M., & Petering, D. H. (1970) *Proc. Natl. Acad. Sci. U.S.A. 67*, 637.
Hoffman, B. M., Diemente, D. L., & Basolo, F. (1970) *J. Am. Chem. Soc. 92*, 61.
Höhn, M. & Hüttermann, J. (1982) *J. Biol. Chem. 257*, 10554.
Hunt, L. T., Hurst-Calderone, S., & Dayhoff, M. O. (1978) in *Atlas of Protein Sequence and Structure* (Dayhoff, M. O., Ed.), 5th ed., pp 229–249, National Biomedical Research Foundation, Washington, DC.
Ikeda-Saito, M., Iizuka, T., Yamamoto, H., Kayne, F. J., & Yonetani, T. (1977) *J. Biol. Chem. 252*, 4882.
Ikeda-Saito, M., Hori, H., Inubushi, T., & Yonetani, T. (1981) *J. Biol. Chem. 256*, 10267.
Imamura, T., Riggs, A., & Gibson, Q. H. (1972) *J. Biol. Chem. 247*, 521.
Jiang, F., McCracken, J., & Peisach, J. (1990) *J. Am. Chem. Soc. 112*, 9035.
Johnson, R. N., Bradbury, J. H., & Appleby, C. A. (1978) *Biol. Chem. 253*, 2148.
Lee, H. C., Ikeda-Saito, M., Yonetani, T., Magliozzo, R. S., & Peisach, J. (1992) *Biochemistry 31*, 7274.
Magliozzo, R. S., McCracken, J., & Peisach, J. (1987) *Biochemistry 26*, 7923.
Martin, K. D., Saari, L., Wang, G.-X., Wang, T., Parkhurst, L. J., & Klucas, R. V. (1990) *J. Biol. Chem. 265*, 19588.
Maurice, A. M. (1981) Ph.D. Thesis, University of Illinois, Urbana, IL.
McCracken, J., Peisach, J., & Dooley, D. M. (1987) *J. Am. Chem. Soc. 109*, 4064.
Mims, M. P., Porras, A. G., Olson, J. S., Noble, R. W., & Peterson, J. A. (1983) *J. Biol. Chem. 258*, 14219.
Mims, W. B. (1974) *Rev. Sci. Instrum. 45*, 1583.
Mims, W. B. (1984) *J. Magn. Reson. 59*, 291.
Mims, W. B., & Peisach, J. (1978) *J. Chem. Phys. 69*, 4921.
Nicola, N. A., Minasian, E., Appleby, C. A., & Leach, S. J. (1975) *Biochemistry 14*, 5141.
Nilges, M. J. (1979) Ph.D. Thesis, University of Illinois, Urbana, IL.
Ollis, D. L., Wright, P. E., Pope, J. M., & Appleby, C. A. (1981) *Biochemistry 20*, 587.
Ollis, D. L., Appleby, C. A., Colman, P. A., Cutten, A. E., Guss, J. M., Venkatappa, M. P., & Freeman, H. C. (1983) *Aust. J. Chem. 36*, 451.
Olson, J. S., Mathews, A. J., Rohlfs, R. J., Springer, B. A., Egeberg, K. D., Sligar, S. G., Tame, J., Renaud, J.-P., & Nagai, K. (1988) *Nature 336*, 265.
Pauling, L. (1964) *Nature 203*, 182.
Peisach, J., Mims, W. B., & Davis, J. L. (1979) *J. Biol. Chem. 254*, 12379.
Phillips, S. E. V., & Schoenborn, B. P. (1981) *Nature 292*, 81.
Pregosin, P. S., Randall, E. W., & White, A. I. (1971) *J. Chem. Soc., Chem. Commun.*, 1602.
Rousseau, D. L., Ondrias, M. R., La Mar, G. N., Kong, S. B., & Smith, K. M. (1983) *J. Biol. Chem. 258*, 1740.
Tovrog, B. S., Kitko, D. J., & Drago, R. S. (1976) *J. Am. Chem. Soc. 98*, 5144.
Trewhella, J., & Wright, P. E. (1979) *Nature 280*, 87.
Trewhella, J., & Wright, P. E. (1980) *Biochim. Biophys. Acta 625*, 202.
Trewhella, J., Wright, P. E., & Appleby, C. A. (1979) *Biochem. Biophys. Res. Commun. 88*, 713.
Wittenberg, J. B., Appleby, C. A., & Wittenberg, B. A. (1972) *J. Biol. Chem. 247*, 527.
Wright, P. E., & Appleby, C. A. (1977) *FEBS Lett. 78*, 61.
Yamamoto, H., Kayne, F. J., & Yonetani, T. (1974) *J. Biol. Chem. 249*, 691.
Yonetani, T. (1967) *J. Biol. Chem. 242*, 5008.
Yonetani, T., Yamamoto, H., & Woodrow, G. V., III (1974) *J. Biol. Chem. 249*, 682.